



Adsorption of carbendazim pesticide on plasmonic nanoparticles studied by surface-enhanced Raman scattering



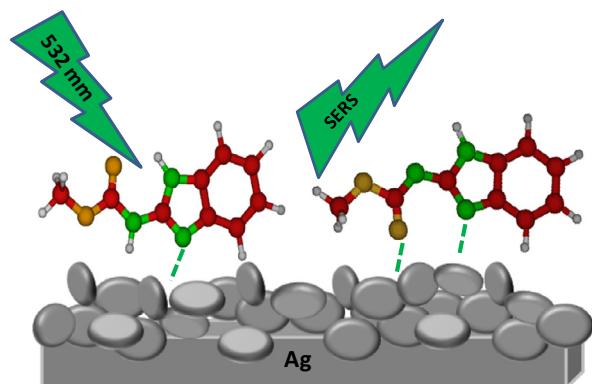
L.N. Furini^a, C.J.L. Constantino^a, S. Sanchez-Cortes^b, J.C. Otero^c, I. López-Tocón^{c,*}

^a FCT, Universidade Estadual Paulista, Presidente Prudente, SP, Brazil

^b Instituto de Estructura de la Materia, CSIC, Serrano 121, E-28006 Madrid, Spain

^c Department of Physical Chemistry, Faculty of Science, University of Málaga, Unidad Asociada CSIC, E-29071 Málaga, Spain

GRAPHICAL ABSTRACT



ARTICLE INFO

Article history:

Received 9 June 2015

Revised 18 November 2015

Accepted 20 November 2015

Available online 21 November 2015

Keywords:

SERS spectroscopy

Adsorption on colloidal suspension

Carbendazim

ABSTRACT

Surface-Enhanced Raman Spectra (SERS) of methyl N-(1H-benzimidazol-2-yl)carbamate (MBC), usually named carbendazim, have been recorded on silver colloids at different pH values. In order to identify the neutral, protonated or deprotonated species of MBC that originate the SERS, the vibrational wavenumbers of these three isolated forms and linked to a silver atom have been predicted by carrying out DFT calculations. The results indicate that the active SERS species in the studied pH range correspond to the neutral MBC and its deprotonated ion in the amidate form. According to theoretical calculations, neutral MBC is linked to the metal through the imidazolic nitrogen atom, while the deprotonated MBC could be linked through the imidazolic nitrogen together with the amidic nitrogen atom or the carbonyl oxygen atom. Both adsorbed species, neutral and deprotonated, have the benzimidazolic ring orientated almost perpendicular to the silver surface and no molecular reorientation has been detected. pH of the bulk controls the relative abundance of the neutral MBC and its amidate anion which can be monitored through the intensities of the SERS bands recorded at about 1230 and 1270 cm^{-1} . These two key bands correspond to the in-plane NH deformation of amidic and imidazolic groups, respectively.

© 2015 Elsevier Inc. All rights reserved.

1. Introduction

Benzimidazole derivatives are heterocyclic compounds of great interest for their technological [1], medical [2] and biological [3]

* Corresponding author.

E-mail address: tocon@uma.es (I. López-Tocón).

applications. Despite the usefulness of these compounds as fungicides and pesticides of broad-spectrum efficacy [4], some of them are classified as pollutants by European Union establishing their concentration limit in different samples. This is the case of methyl N-(1H-benzimidazol-2-yl)carbamate (MBC), usually named carbendazim. MBC is a systemic fungicide, white powder, with very low solubility in water ~ 6.11 mg/L. It has two pK_a ($pK_{a1} = 4.5$ and $pK_{a2} = 10.6$) controlling the relative abundance of protonated (MBC^+), neutral (MBC^0) and deprotonated (MBC^-) forms in aqueous solution, depending on the pH (Fig. 1) [5].

Several analytical methods have been proposed to identify and quantify the presence of environmental pollutants [6,7], as for example, the spectroscopic technique Surface-Enhanced Raman Scattering (SERS) [8,9]. SERS is nowadays used for sensitive and selective molecular identification due to the giant electromagnetic (EM) enhancement of the Raman signal induced by localized plasmon resonances in nanostructured noble metal surfaces [10,11]. This huge enhancement provide strong Raman signals from very insoluble compounds such as MBC [5] and allows, for instance, to record the spectra of hydrophobic molecules in aqueous solution at trace level by using molecular hosts of specific analytes such as viologen dications [9,12] or cyclodextrins [13] among others.

Beside analytical applications as chemical sensor, SERS is also a powerful tool to gain insight into the nature of the metal-adsorbate hybrid, the bonded molecular species and its chemical interaction with the metal nanostructure [14–16]. SERS spectra of simple molecules related to MBC such as benzimidazole (BIZ) [16] and imidazole (IZ) [15] have been previously studied. In the case of BIZ two different types of adsorption are proposed depending on the pH, through the π -electrons of the aromatic ring at neutral pH or through the protonated nitrogen atom at acidic pH that assembles a strong ionic pair with chlorine anion [16]. A similar change in the adsorption was found in the case of cyanide anion where a molecular reorientation from perpendicular to parallel adsorption occurs when the cyanide concentration is lowered [17]. Even in the case of acidic pH, the adsorption through deprotonated nitrogen cannot be discarded given the strong chemical interaction between the lone pair of the heteroatom and the metal as well as the effective pH in the interface of a nanometric environment which can be far apart from the bulk values [18].

MBC is a much more complex adsorbate given that three different chemical species have to be considered depending on the pH: the neutral molecule (MBC^0) and the protonated (MBC^+) and the deprotonated (MBC^-) charged species. Both ionic forms are stabilized by resonance because of the positive or negative charge can be delocalized along the aromatic heterocyclic ring and the carbamate group (Fig. S1 in Supplementary Material). This effect slightly increases the basicity of the imidazolic nitrogen ($pK_{a1} = 4.5$) with respect to other compounds with sp^2 hybridization [19] although remains less basic than imidazole ($pK_a = 7.0$), aliphatic amines ($pK_a = 10–11$) or ammonia ($pK_a = 9.24$). On the other hand, the amidic nitrogen atom located in the carbamate group is slightly more acid ($pK_{a2} = 10.6$) than aliphatic amides ($pK_a = 14–15$) [19].

This work is mainly focused on the study of the effect of the pH in the coordination of a complex molecular system like MBC on

metallic plasmonic surfaces by means of SERS in order to identify the adsorbed species and the specific interacting center with the metal. In this way, SERS spectra of 10^{-5} mol/L MBC have been recorded on silver sols at several pH values ranging from pH = 2 up to 12. The analysis of the results has been carried out with the help of Density Functional Theory (DFT) calculations which have proved once again their usefulness in the spectral interpretation.

2. Methods

All reagents and MBC were purchased from Sigma–Aldrich. Stock solutions (10^{-3} mol/L) of MBC were prepared with ethanol (100%) provided by VWR, Prolab. Silver sols and aqueous solutions were prepared with water from Milli-Q system (18.2 M Ω cm resistivity).

2.1. Preparation of Ag nanoparticles and SERS measurements

Ag nanoparticles (AgNPs) were prepared by reducing an aqueous solution of silver nitrate (10^{-2} mol/L) with hydroxylamine hydrochloride (1.66×10^{-3} mol/L) in alkaline medium (300 μ L NaOH 1.0 mol/L) under vigorous stirring according to the procedure described elsewhere [20,21]. Other reducing agents such as citrate and $NaBH_4$ can be alternatively used to obtain colloidal suspensions, but it has been shown that the NPs obtained by using hydroxylamine show a more uniform distribution of size and shape and no interferences from the remaining oxidation products are detected [22]. AgNPs were characterized by the resonances of metallic plasmons in the UV–VIS spectra, showing a maximum at about 410 nm with an average FWHM of 80 nm, and by SEM (Fig. S2 in Supplementary Material). Although the NPs are partially aggregated, there are no large clusters and the isolated NP diameter is of ca. 50 nm. This size is similar to that measured by dynamic light scattering, 54 nm. The zeta potential has been also measured yielding a value of -30.5 mV. Both parameters (size and zeta potential) agree quite well with the characteristic values of electrostatically stabilized sols [23]. A NanoBrook ZetaPALS analyzer with a 35 mW red diode laser, nominal 640 nm wavelength, has been employed to measure the diameter and the zeta potential of AgNPs and a Hitachi S-4800 FESEM instruments for obtaining SEM images.

Different procedures to prepare the final samples have been checked in order to optimize the SERS signal/noise ratio. AgNPs colloids were activated by adding 40 μ L KNO_3 (0.5 mol/L) to 960 μ L of AgNPs in a 1 cm \times 1 cm cuvette. The final pH of the colloid was adjusted by adding 5 μ L HNO_3 (1.0 mol/L) for obtaining pH = 2, and 0.5, 1, 1.5 and 5 μ L NaOH of 0.5, 1.0, 1.0 and 2.0 mol/L, respectively, for obtaining the corresponding pH of 6, 8, 10 and 12, respectively. The pre-aggregation induced by KNO_3 leads to a slight change of the color as well as an enhancement of the plasmon absorption at higher wavelengths as described in Supplementary Material. Finally, an aliquot of 10 μ L was removed from the mixture and 10 μ L of MBC solution (10^{-3} mol/L) was added in

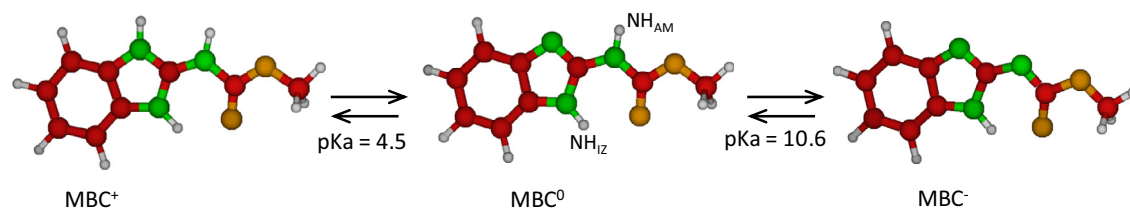


Fig. 1. B3LYP/6-31G* optimized structures of different chemical species of MBC that can exist in aqueous solution depending on the pH.

order to keep the volume in 1000 μL . The final MBC concentration was 10^{-5} mol/L in all experiments. The pH values have been measured by pH-indicator strips (MColorpHast, Merck) after adding MBC molecule. The uncertainty of the measured pH is estimated to be ± 0.5 (pH = 5–10) or ± 1 (pH = 0–5 and 10–14). pH has a minimal effect on the stability of the sols in the studied range and the ionic strength remains almost kept constant in all the samples. The stability of the colloid is discussed within [Supplementary Material \(Figs. S3 and S4\)](#).

Raman spectra were obtained using a micro-Raman inVia Renishaw spectrograph, equipped with an electrically cooled CCD camera, under 532 nm excitation and diffraction grating of 1800 l/mm. The laser power reaching the sample was about 2.0 mW and the spectral resolution was set to 2 cm^{-1} . Raman spectrum of powder was recorded using the 785 nm exciting line to avoid fluorescence emission. Although absolute SERS intensity can slightly vary on a particular record, the relative SERS intensity of the bands keeps constant. SERS spectra have been repeated several times under the same experimental conditions in order to check the reproducibility of the intensity ratio of the key bands at 1230 and 1270 cm^{-1} and estimating a reproducibility similar to that found in the previous work (ca. <20% [9]).

UV/Vis spectra have been recorded on a Cintra 5 double beam spectrophotometer dotted with Tungsten-halogen and deuterium lamps and 1.5 nm slit width. The samples were prepared in the same way to that mentioned for recording SERS spectra. The only difference is that the sample (1 mL) was diluted with 2 mL of ultra-pure water (Milli-Q system) in order to avoid the spectral saturation.

2.2. Theoretical calculations

Optimized structure and force field of neutral MBC^0 , BIZ and IZ were calculated at B3LYP/6-31G* level of theory. It has been demonstrated that this level of calculation reproduces satisfactorily the vibrational spectrum of aromatic molecules [24,25]. Geometry optimization of MBC^0 has been constrained to a planar structure (C_s symmetry) where an intramolecular hydrogen bond occurs between the imidazolic NH bond and the amidic oxygen atom. This MBC^0 structure agrees with the local symmetry in solid phase, providing a higher crystallinity than BIZ [26], a lower solubility in water as well as a higher melting point of MBC in comparison to BIZ [13]. The optimized structure of protonated and deprotonated MBC, (MBC^+ and MBC^- , respectively) and their corresponding vibrational wavenumbers have also been calculated. [Fig. 1](#) shows the B3LYP/6-31G* optimized geometry of the MBC species and summarizes the nomenclature used for the two different NH bonds: imidazolic NH_{IZ} and amidic NH_{AM} .

In addition, a simple molecular model has been assumed for the MBC–Ag surface complex involving a single silver atom linked to the three different chemical species of MBC ([Fig. 2](#)). A positive or negative silver atom has been selected depending of the negatively/neutral or positively charged MBC forms, respectively, in order to minimize the electrostatic repulsion between the AgNP and the adsorbate because of larger SERS enhancement is detected under this condition [27]. B3LYP method with the LanL2DZ basis set has been employed for calculating the respective optimized structures and force fields of the different complexes ($\text{MBC}^0\text{-Ag}^+$, $\text{MBC}^+\text{-Ag}^-$, $\text{MBC}^-\text{-Ag}^+$). This is the same level of calculation previously used by us for analyzing the adsorption and charge transfer processes in the SERS of benzene-like molecules [28,29]. The silver cation is bonded to the imidazolic or the amidic nitrogen atoms in the optimized complexes of MBC^0 or MBC^- species, respectively, as occurs in heterocyclic aromatic molecules where the nitrogen atom is preferred to adsorb on the metallic surface [30,31]. In the case of MBC^+ , the only available interaction with silver is through

the π -system of the aromatic rings given that all the nitrogen atoms are bonded to hydrogen. As expected, the $\text{MBC}^+\text{-Ag}^+$ complex dissociates in the optimization process. Therefore, a negatively charged silver atom has been considered in order to predict the vibrational wavenumbers associated to this species ($\text{MBC}^+\text{-Ag}^-$). All the calculated wavenumbers of the different complexes are real indicating that the optimized geometries correspond to equilibrium structures ([Table S1 in Supplementary Material](#)) and no scaling factor was used for the force field given that the accuracy of B3LYP vibrational wavenumbers are typically better than 95% of the experimental values [32]. All calculations have been carried out using the GAUSSIAN09 program package [33].

3. Results and discussion

3.1. SERS spectra of carbendazim at different pH

Raman spectrum of solid MBC ([Fig. S5 in Supplementary Material](#)) has been recorded giving that the low solubility of MBC prevents recording the Raman from aqueous solutions at any pH. This spectrum is dominated by seven strong bands recorded at 1475, 1271, 1262, 1030, 961, 724 and 618 cm^{-1} as well as two very strong bands at lower wavenumbers (<150 cm^{-1}) which correspond to lattice vibrations. The remaining bands recorded in the 200–1800 cm^{-1} region show a much lower intensity than the previous ones. [Table S2 \(Supplementary Material\)](#) shows the vibrational assignment of MBC taking into account the B3LYP/6-31G* force field of the isolated chemical species and the reported assignment [34–39] of related molecules. The bands associated to the amidic and imidazolic NH bonds have been highlighted. The 1200–1300 cm^{-1} region is very interesting in order to recognize the presence of a particular ionized form of MBC given that characteristic bands of specific deprotonated species are recorded at these wavenumbers.

[Figs. 3 and 4](#) show the medium and high wavenumber regions, respectively, of SERS spectra of MBC recorded at different pH values. All the spectra have been normalized to the corresponding strongest band, except for the weak SERS at pH = 2 which shows a very strong background. SERS at pH = 6 is almost identical to that at pH = 8 and both spectra are dominated by five strong SERS bands recorded at about 1520, 1460, 1270, 1230 and 1010 cm^{-1} . However, in the SERS at pH = 10 the relative intensities of the doublets appearing at 1230/1270 cm^{-1} ([Fig. 3](#)) and 2950/3070 cm^{-1} ([Fig. 4](#)) are reversed. As a consequence, the bands at 1270 and 2950 cm^{-1} become the strongest ones of the respective pairs when the pH is basic enough. The dependence of the relative intensities of these bands on the pH can be related to the normal modes of the functional group which undergoes deprotonation, i.e. the amidic NH group, and therefore, these bands can be used to recognize which MBC chemical species (neutral or ionized) is adsorbed on the basis of the force field calculations.

3.2. Vibrational assignment of MBC

The analysis of the vibrational and SERS spectra of a complex molecular system such as MBC has been carried out on the basis of the force field calculations and the assignments of BIZ [16,34] and IZ [15,35–37] related molecules. [Table S2 \(Supplementary Material\)](#) correlates the experimental Raman wavenumbers of solid MBC and those of BIZ and IZ together with those calculated by using the B3LYP/6-31G* method for all the considered chemical species. [Table S3 \(Supplementary Material\)](#) summarizes in turn the SERS wavenumbers of MBC recorded at different pH values and the

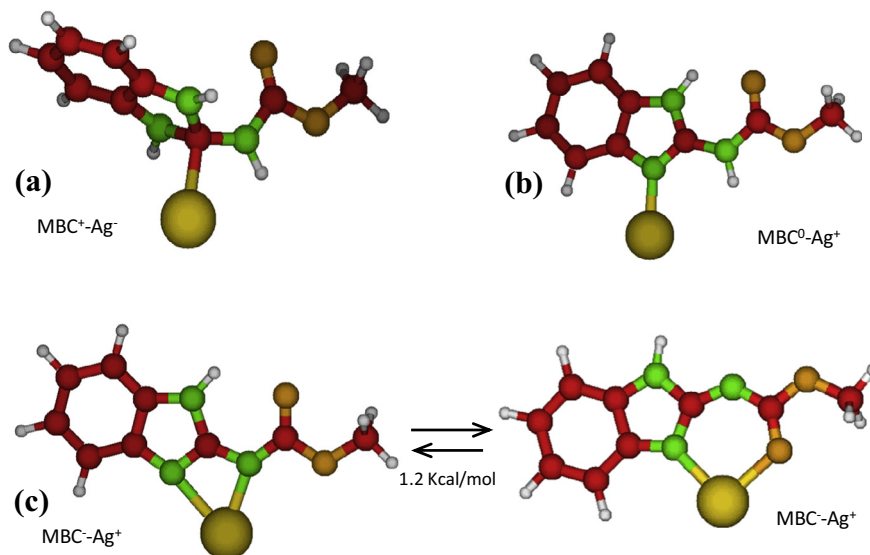


Fig. 2. B3LYP/LanL2DZ optimized structures of (a) MBC^+-Ag^- , (b) MBC^0-Ag^+ and (c) MBC^--Ag^+ (Left: N–Ag–N; Right: N–Ag–O) surface complexes and energy difference between the two optimized structures of the MBC^--Ag^+ complex, being slightly more stable the complex in which the silver atom is linked to both the imidazolic nitrogen and the oxygen of the carbamate group (right).

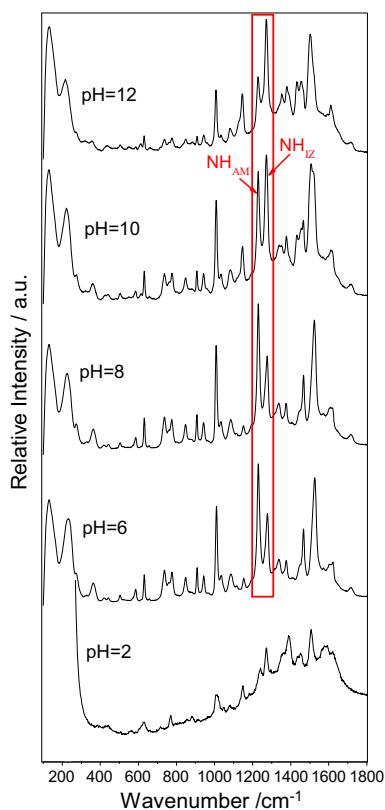


Fig. 3. SERS spectra of MBC (10^{-5} mol/L) recorded at different pH values under 532 nm excitation.

B3LYP/LanL2DZ theoretical ones for the different MBC–Ag surface complexes.

The strongest SERS bands (Fig. 3) are assigned to in-plane normal modes and only few lines correspond to out-of-plane fundamentals. The five strong SERS bands recorded at about 1520, 1460, 1270, 1230 and 1010 cm^{-1} at $\text{pH} \geq 6$ are assigned to vibrational motions involving mainly $\delta\text{NH}_{\text{AM}}$, $\delta\text{NH}_{\text{AM}} + \delta\text{CH}_3$, $\delta\text{NH}_{\text{IZ}}$,

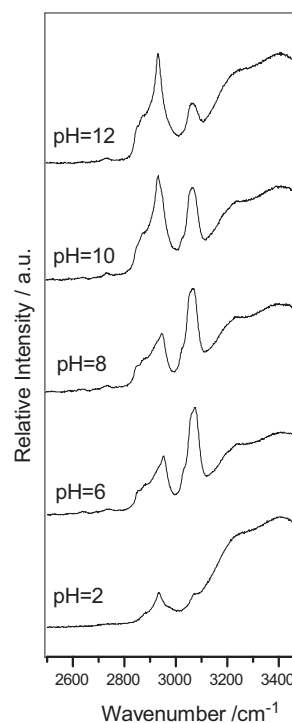


Fig. 4. High wavenumber region of SERS spectra of MBC (10^{-5} mol/L) recorded at different pH values under 532 nm excitation.

$\delta\text{NH}_{\text{AM}}$ and $\delta\text{CC}_{\text{BZ}}$ in-plane deformations, respectively. The characteristic vibrational modes of the amide group have also been identified. Amide I vibration, recorded at about 1650 cm^{-1} , arises mainly from the C=O stretching coordinate, and the Amide II band, recorded at about 1550 cm^{-1} , corresponds to a combination of the NH_{AM} in-plane bending and the CN stretching coordinates. Although this last band is usually weak or absent in the Raman spectrum of polypeptides, the medium-strong SERS band observed at 1520 cm^{-1} can be assigned to Amide II. This band splits in two components at $\text{pH} = 10$, 1520 and 1507 cm^{-1} , being that recorded

at 1520 cm^{-1} slightly weaker than the new one at 1507 cm^{-1} and, finally, becomes very weak appearing as a shoulder at $\text{pH} = 12$. The force field predicts one or two fundamentals in this region, depending of the considered MBC^- or MBC^0 species, at 1528 and 1542 cm^{-1} and assigned to NH_{IZ} and NH_{AM} in-plane deformations, respectively (Table S3, Supplementary Material). The Amide III vibration of MBC, recorded with strong intensity at 1230 cm^{-1} , corresponds to a combination of NH_{AM} bending and CC benzenic stretching coordinates. Another strong SERS band is appearing at 1270 cm^{-1} which contains a large contribution from NH_{IZ} in-plane deformation.

There are also a couple of bands recorded over 1400 cm^{-1} showing a similar behavior to that described for the 1200 and 1500 cm^{-1} regions, that is, their relative intensities are reversed at basic pH in agreement with the proposed assignment, giving that both fundamentals are related to the NH_{AM} and NH_{IZ} in-plane deformations.

Regarding the high wavenumber region, two broad SERS bands are recorded in all spectra at about 3400 and 3200 cm^{-1} , respectively, where NH (adsorbate, Fig. 4) and OH (water, Figs. 4 and S4) stretching vibrations are overlapped. Two bands appear at lower wavenumbers, 3070 and 2950 cm^{-1} , whose relative intensities are sensitive to the pH and showing a reverse dependence to those recorded at 1230 and 1270 cm^{-1} . This point out to these bands should be also related to the relative abundance of the neutral and anionic species, MBC^0 and MBC^- respectively. We propose two alternative explanations for the dependence of their intensities on the pH. It is possible that both bands are originated by a Fermi resonance involving a CH stretching fundamental and the overtone of the Amide II band (recorded, for instance at 1523 cm^{-1} in the SERS at $\text{pH} = 6$ (MBC^0 , $2 \times 1523 = 3046\text{ cm}^{-1}$)) as occurs in similar compounds like in proteins [38,40]. Another possibility is that both bands correspond to aromatic and methyl CH stretching vibrations which are expected to appear above and below 3000 cm^{-1} , respectively. The relative enhancement of the band corresponding to the alkyl CH (2950 cm^{-1}) at higher pH could be due to the closer proximity of the methyl group to the metal surface in the case of the MBC^- -Ag⁺ complex (Fig. 2c) than in the case of the MBC^0 -Ag⁺ complex (Fig. 2b), where the silver is displaced toward the aromatic moiety, which could be responsible for the strong intensity of the 3070 cm^{-1} SERS line at $\text{pH} = 6$.

3.3. Adsorption of MBC on Ag nanoparticles

The analysis of the B3LYP/LanL2DZ calculated wavenumbers of the three different Ag-MBC surface complexes (MBC^0 -Ag⁺, MBC^- -Ag⁺, MBC^+ -Ag⁻, Fig. 2 and Table S3) indicates that the main changes should correspond to the fundamentals related to the ionizable imidazolic and amidic groups. Generally speaking, the interaction of the imidazole ring with the surface seems to dominate the adsorption of MBC on silver, even in the case of neutral MBC^0 , as pointed out by the calculated fundamentals at 1027 and 1363 cm^{-1} of the complex with Ag⁺.

In addition, most of the enhanced bands in the SERS spectrum, such as those recorded at ca. 1520 , 1270 , 1230 and 1010 cm^{-1} , correspond to in-plane normal modes of aromatic rings what suggests a perpendicular orientation of the benzimidazolic ring with respect to the metallic surface on the basis of the propensity rules of the EM enhancement mechanism of SERS [41]. Although some of the single bonds related to the carbamate group could rotate more or less freely (giving “non-planar” conformations), the presence of a hydrogen bond in the carbamate (see Fig. 2b and c), the resonance in the amide group and the bonding with the silver favors a C_s structure with perpendicular orientation of the adsorbate. Only internal rotations along the C–O(CH₃) and O–CH₃ single bonds are expected. In addition, B3LYP/LanL2DZ calculations predict a

molecular structure for MBC^0 -Ag⁺ and the two conformers of MBC^- -Ag⁺ with C_s symmetry in which two equivalent methyl hydrogens lie above and below the symmetry plane (Table S1 in Supplementary Material).

The chemical species adsorbed on the silver surface can be checked by analyzing the dependence on the pH of the relative SERS intensities of the pairs of the bands assigned to amidic/imidazolic groups. The most striking feature is the behavior of the bands recorded at $1230/1270\text{ cm}^{-1}$ and assigned to NH_{AM} and NH_{IZ} in-plane deformations, respectively, where the relative intensity of the 1230 cm^{-1} line decreases when pH increases, while the 1270 cm^{-1} band becomes in turn stronger. There are also other bands sensitive to the pH recorded in the 1300 and 1400 cm^{-1} region as, for instance, the bands assigned to the amidic group (1340 and 1460 cm^{-1}) that become weaker than the assigned to imidazolic group (1380 and 1430 cm^{-1}) when the pH is raised. The same occurs in the 1500 cm^{-1} region. The band recorded at 1522 cm^{-1} (amidic group) shows a shoulder at 1505 cm^{-1} (imidazolic group) in the SERS at $\text{pH} = 10$ and dominates at $\text{pH} = 12$. These results indicate that the MBC^0 and MBC^- chemical species are adsorbed on the nanoparticles and that the MBC^+ species is not able to interact with the surface. The imidazolic N atom is involved in the adsorption process and only when MBC^0 species is present in the sol ($\text{pH} > 6$) an enhancement of SERS intensity is observed. This is also observed in the VIS spectra of MBC colloidal solutions measured at different pH (Fig. 5). A new band at high wavelength ($\approx 780\text{ nm}$), and characteristic of aggregation, appears in the spectra at $\text{pH} > 6$, indicating that the adsorption of MBC on AgNPs is only effective when the pesticide is in neutral or anionic forms, thus corroborating that the IZ group is involved in the interaction with the metal. These evidences, together with the absence of any SERS band recorded at ca. 1295 cm^{-1} which is assigned to NH deformation of the protonated imidazolic nitrogen (see Table S3), corroborates that MBC^0 or MBC^- species originate the SERS.

This conclusion is further supported by the attempts to calculate the optimized B3LYP/LanL2DZ geometry of the MBC^+ -Ag⁺. These calculations do not converge to any minimum given that the MBC^+ cation does not have any free nitrogen atom able to interact with the metallic surface. Only an optimized geometry for the MBC^+ -Ag⁻ complex has been obtained where the negatively charged silver atom is located above the aromatic ring (see Fig. 2a). In this case, the MBC^+ loses the planarity because of the imidazolic carbon pyramidalizes while the silver anion is located above the three nitrogen atoms. This kind of interaction would give rise to the enhancement of SERS bands corresponding to the

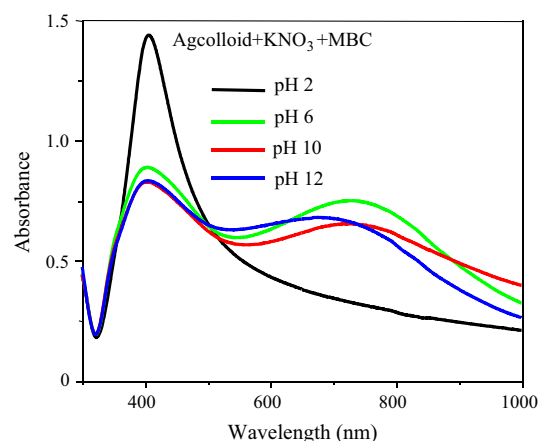


Fig. 5. UV-Vis absorption spectra of Ag sols with KNO_3 and MBC at different pH values.

out-of-plane normal modes of the aromatic rings [41] but no bands assigned to these vibrations are enhanced, what discards the adsorption of the cationic MBC^+ species.

Therefore, MBC^0 and its amidate anion MBC^- are the two chemical species adsorbed on the metallic surface. The optimized structure of the $\text{MBC}^0\text{-Ag}^+$ complex yields a planar geometry with C_s symmetry, where the silver atom is bonded to the imidazolic nitrogen atom giving a perpendicular orientation of the benzimidazolic ring with respect to the metallic surface (Fig. 2b). The calculated vibrational wavenumbers for this complex are in agreement with the experimental ones. The MBC^- species contains the amidate group and can be adsorbed through either the imidazolic and the amidic nitrogen atoms (N–Ag–N), or the imidazolic nitrogen and the carbonyl oxygen atom (N–Ag–O) as show the corresponding optimized structures (Fig. 2c). The calculated force fields for both metallic complexes predict very similar wavenumbers in agreement with the experimental results and the energy difference between these two structures is very small (1.2 kcal/mol), being the last complex slightly more stable.

As a result from the analysis of the vibrational assignment based on the force field calculations (Table S3) it can be concluded that the 1230 and 1270 cm^{-1} SERS bands are characteristic of the neutral and ionic $\text{MBC}^0/\text{MBC}^-$ species, respectively, as the respective dependence of their intensities on the pH shows. In this respect, we have found a linear correlation between the intensity ratio of these SERS bands I_{1230}/I_{1270} (measured from their peak heights) and the pH as shows Fig. 6 what allows for predicting (at least roughly) macroscopic pH value of the solution from the relative intensities of both bands. This linear dependence has been already observed in molecules that show an ionizable group and a surface interacting center, what allows for using them as pH-sensor [42]. On the contrary, simple carboxylic acids or amides are no valid pH SERS-sensors because the ionizable chemical group is also involved in the linkage with the metal [18].

4. Conclusions

The identification of the chemical species of MBC adsorbed on Ag nanoparticles has been carried out on the basis of DFT quantum mechanical calculations and by analyzing the dependence of the SERS spectra on the pH. A complete vibrational assignment of all the possible chemical species adsorbed on the silver surface has been proposed. The SERS active forms correspond to the neutral MBC and its amidate ion (MBC^-) with a perpendicular orientation of the benzimidazolic ring with respect to the metallic surface, given that no out-of-plane bands are enhanced in SERS. The

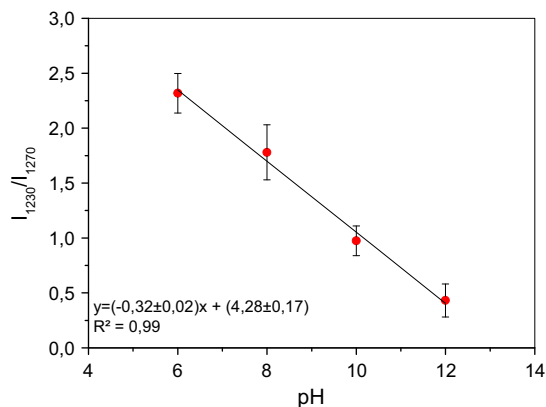


Fig. 6. Dependence of the relative intensity of the SERS bands recorded at 1230 and 1270 cm^{-1} on the pH.

changes in the intensities of the pairs or SERS bands recorded in the 1200 cm^{-1} and 3000 cm^{-1} regions when the pH is raised evidence the relative concentration of neutral/amidate species. Moreover, theoretical results point out that the MBC coordination to Ag surface is monodentate through the imidazolic nitrogen atom in neutral MBC species and bidentate through both imidazolic and amidic nitrogen atoms or the oxygen atom of the amidate group in MBC^- anionic species. Finally a linear dependence between the relative intensity of the 1230/1270 cm^{-1} bands on the pH has been found because of the amide group is not involved in the adsorption process.

Acknowledgments

We are grateful to the Spanish MINECO (CTQ2012-31846, FIS2014-52212-R) and Junta de Andalucía (FQM-5156 and 6778), and to the Brazilian agencies CAPES, CNPq and FAPESP, for financial support. The authors thank to SCAI and Rafael Larrosa (UMA) for computational facilities.

Appendix A. Supplementary material

Fig. S1 shows the resonance structures of MBC^+ and MBC^- ions, and Figs. S2–S4 correspond to the SEM image of AgNPs, UV–Vis spectra of colloid, pre-aggregated colloid and aggregated with the adsorbate MBC, and the Raman spectra of pre-aggregated colloid at different pH, respectively. Fig. S5 shows the Raman spectrum of solid MBC. Table S1 summarizes the Cartesian coordinates of the different complexes and Tables S2 and S3 summarize in turn the experimental (Raman and SERS) and theoretical DFT vibrational wavenumbers of BIZ, IZ and MBC and the calculated silver complexes. Supplementary data associated with this article can be found, in the online version, at <http://dx.doi.org/10.1016/j.jcis.2015.11.045>.

References

- [1] Y. Tang, F. Zhang, S. Hu, Z. Cao, Z. Wu, W. Jing, *Corros. Sci.* 74 (2013) 271.
- [2] S. Bhattacharya, P. Chaudhuri, *Curr. Med. Chem.* 15 (2008) 1762.
- [3] M. Lezcano, W. Al-Soufi, M. Novo, E. Rodríguez-Núñez, J.V. Tato, *J. Agric. Food Chem.* 50 (2002) 108.
- [4] H.S. Zhu, L.H. Wu, R.B. Li, L.A. Xia, J.Q. Han, Q.J. Zhang, Y.C. Bian, Q.R. Yu, *Anal. Chim. Acta* 619 (2008) 165.
- [5] N. Ni, T. Sanghvi, S.H. Yalkowsky, *Int. J. Pharm.* 244 (2002) 99.
- [6] M. Pozo, L. Hernández, C.A. Quintana, *Talanta* 81 (2010) 1542.
- [7] T. Vo-Dinh, J. Fetzer, A.D. Campliglia, *Talanta* 47 (1998) 943.
- [8] L.N. Furini, S. Sanchez-Cortes, I. López-Tocón, J.C. Otero, R.F. Aroca, C.J.L. Constantino, *J. Raman Spectrosc.* (2015), <http://dx.doi.org/10.1002/jrs.4737>.
- [9] I. López-Tocón, J.C. Otero, J.F. Arenas, J.V. Garcia-Ramos, S. Sanchez-Cortes, *Anal. Chem.* 83 (2011) 2518.
- [10] M. Moskovits, *Rev. Mod. Phys.* 57 (1985) 783.
- [11] R. Aroca, *Surface-Enhanced Vibrational Spectroscopy*, John Wiley & Sons, Chichester, U.K., 2006.
- [12] L. Guerrini, J.V. Garcia-Ramos, C. Domingo, S. Sanchez-Cortes, *Anal. Chem.* 81 (2009) 1418.
- [13] P. Leyton, S. Sánchez-Cortes, J.V. Garcia-Ramos, C. Domingo, M. Campos-Valette, C. Saitz, R.E. Clavijo, *J. Phys. Chem. B* 108 (2004) 17484.
- [14] A.K. Ojha, *Chem. Phys.* 340 (2007) 69.
- [15] B.H. Loo, Y. Tse, K. Parsons, C. Adelman, A. El-Hage, Y.G. Lee, *J. Raman Spectrosc.* 37 (2006) 299.
- [16] M.S. Kim, M.K. Kim, C.J. Lee, Y.M. Jung, M.S. Lee, *Bull. Korean Chem. Soc.* 30 (2009) 2930.
- [17] D.S. Kellogg, J.E. Pemberton, *J. Phys. Chem.* 91 (1987) 1120.
- [18] J.L. Castro, M.R. Lopez-Ramirez, J.F. Arenas, J. Soto, J.C. Otero, *Langmuir* 28 (2012) 8926.
- [19] A. Streitwieser, C.H. Heathcock, E.M. Kosower, *Introduction to Organic Chemistry*, Prentice-Hall, 1998.
- [20] L. Guerrini, J.V. Garcia-Ramos, C. Domingo, S. Sanchez-Cortes, *Anal. Chem.* 81 (2009) 953.
- [21] N. Leopold, B. Lendl, *J. Phys. Chem. B* 107 (2003) 5723.
- [22] M.V. Cañamares, J.V. Garcia-Ramos, J.D. Gómez-Varga, C. Domingo, S. Sanchez-Cortes, *Langmuir* 21 (2005) 8546.
- [23] A.M. El Badawy, T.P. Luxton, R.G. Silva, K.G. Scheckel, M.T. Suidan, T.M. Toloyamat, *Environ. Sci. Technol.* 44 (2010) 1260.

- [24] L. Bencivenni, F. Ramondo, V. Pieretti, N. Sanna, *J. Chem. Soc. Perkin Trans. 2* (2000) 1685.
- [25] G.A. Giffin, G.A. Boesch, D.N. Boepe, D.R. Powell, R.A. Wheeler, R. Frech, *J. Phys. Chem. B* 113 (2009) 15914.
- [26] C.J. Dik-Edixhoven, H. Schent, H. Van der Meer, *Cryst. Struct. Commun.* 2 (1973) 23.
- [27] R.A. Alvarez-Puebla, E. Arceo, P.J.G. Goulet, J.J. Garrido, R.F. Aroca, *J. Phys. Chem. B* 109 (2005) 3787.
- [28] S.P. Centeno, I. López-Tocón, J. Roman-Perez, J.F. Arenas, J. Soto, J.C. Otero, *J. Phys. Chem. C* 116 (2012) 23639.
- [29] F. Avila, D.J. Fernandez, J.F. Arenas, J.C. Otero, J. Soto, *Chem. Commun.* 47 (2011) 4210.
- [30] J. Soto, D.J. Fernández, S.P. Centeno, I. López Tocón, J.C. Otero, *Langmuir* 18 (2002) 3100.
- [31] M. Sardo, C. Ruano, J.L. Castro, I. López-Tocón, J. Soto, P. Ribeiro-Claro, J.C. Otero, *Phys. Chem. Chem. Phys.* 11 (2009) 7437.
- [32] Z.Q. Cai, Y.X. Zhu, Y. Zhang, *Spectrochim. Acta, Part A* 69 (2008) 130.
- [33] M.J. Frisch, G.W. Trucks, H.B. Schlegel, G.E. Scuseria, M.A. Robb, J.R. Cheeseman, G. Scalmani, V. Barone, B. Mennucci, G.A. Petersson, H. Nakatsuji, M. Caricato, X. Li, H.P. Hratchian, A.F. Izmaylov, J. Bloino, G. Zheng, J.L. Sonnenberg, M. Hada, M. Ehara, K. Toyota, R. Fukuda, J. Hasegawa, M. Ishida, T. Nakajima, Y. Honda, O. Kitao, H. Nakai, T. Vreven, J.A. Montgomery Jr., J.E. Peralta, F. Ogliaro, M. Bearpark, J.J. Heyd, E. Brothers, K.N. Kudin, V.N. Staroverov, R. Kobayashi, J. Normand, K. Raghavachari, A. Rendell, J.C. Burant, S.S. Iyengar, J. Tomasi, M. Cossi, N. Rega, J.M. Millam, M. Klene, J.E. Knox, J.B. Cross, V. Bakken, C. Adamo, J. Jaramillo, R. Gomperts, R.E. Stratmann, O. Yazyev, A.J. Austin, R. Cammi, C. Pomelli, J.W. Ochterski, R.L. Martin, K. Morokuma, V.G. Zakrzewski, G.A. Voth, P. Salvador, J.J. Dannenberg, S. Dapprich, A.D. Daniels, Ö. Farkas, J.B. Foresman, J.V. Ortiz, J. Cioslowski, D.J. Fox, Gaussian 09, Revision D.01, Gaussian, Inc., Wallingford CT, 2009.
- [34] M.A. Morsy, M.A. Al-Khaldi, A. Suwaiyan, *J. Phys. Chem. A* 106 (2002) 9196.
- [35] C.M. Yoshida, T.B. Freedman, T.M. Loehr, *J. Am. Chem. Soc.* 97 (1975) 1028.
- [36] D.A. Carter, J.E. Pemberton, *Langmuir* 8 (1992) 1218.
- [37] M. Majoube, M. Henry, L. Chinsky, P.Y. Turpin, *Chem. Phys.* 169 (1993) 231.
- [38] S. Krimm, J. Bandekar, *Adv. Protein Chem.* 38 (1986) 181.
- [39] A. Barth, C. Zscherp, *Quart. Rev. Biophys.* 35 (2002) 369.
- [40] J. Bellanato, *J. Spectrochim. Acta* 16 (1960) 1344.
- [41] M. Moskovits, D.P. DiLella, K.J. Maynard, *Langmuir* 4 (1988) 67.
- [42] S.W. Bishnoi, C.J. Rozell, C.S. Levin, M.K. Gheith, B.R. Johnson, D.H. Johnson, N.J. Halas, *Nano Lett.* 6 (2006) 1687.